

Postcollision recapture in the K -shell photodetachment of Li^-

T. W. Gorczyca,¹ O. Zatsarinny,¹ H.-L. Zhou,² S. T. Manson,² Z. Felfli,³ and A. Z. Msezane³

¹*Department of Physics, Western Michigan University, Kalamazoo, Michigan 49008, USA*

²*Department of Physics and Astronomy, Georgia State University, Atlanta, Georgia 30303, USA*

³*Center for Theoretical Studies of Physical Systems, Clark Atlanta University, Atlanta, Georgia 30314, USA*

(Received 3 April 2003; published 17 November 2003)

A fully quantum-mechanical modification to the R -matrix method is introduced to include the recapture of slow photoelectrons following Auger decay of an inner-shell vacancy state and is applied to the photodetachment of Li^- above the $1s^{-1}$ threshold. The results show excellent agreement with experiment and resolve a large discrepancy in the cross section near the $1s$ threshold between theory and experiment.

DOI: 10.1103/PhysRevA.68.050703

PACS number(s): 32.80.Gc

Negative ions are ideal systems for probing many-body interactions among atomic electrons [1]. An outer bound or detached electron does not propagate in a long-range Coulomb potential and, therefore, the complicated interactions with the neutral-atom core are not overshadowed. Inner-shell electron detachment in negative ions is even more interesting because of the dramatic relaxation of outer electrons and the subsequent Auger decay of the inner-shell vacancy atom, giving rise to the so-called postcollision interaction (PCI) [2,3] between the photoelectron and the Auger electron.

Photodetachment spectroscopy provides a particularly efficient means for probing atoms in great detail. Earlier, *all* photodetachment studies considered only outer-shell processes. Quite recently, however, measurements of inner-shell photodetachment have been performed for He^- [4], Li^- [5,6], and C^- [7] where synchrotron radiation was required in order to detach the more tightly bound $1s$ electrons. Furthermore, only positive ions, i.e., only channels having both photoelectron and Auger-electron ejection, were detected. Thus, the measured cross sections were subject to postcollision interaction effects between the photoelectron and the Auger electron, which can alter the cross section.

To accurately calculate the shape resonance and relaxation behavior of inner-shell photodetachment, sophisticated theoretical techniques beyond an independent-particle, Hartree-Fock approach are necessary. The R -matrix method [8], being a coupled-channel, flexible basis approach, is one such tool that is used to reproduce observed photodetachment spectra, thereby unraveling the important electron interactions at play.

While R -matrix calculations for inner-shell photodetachment of He^- [9], Li^- [5,10], and C^- [7] have generally shown good agreement with the experimental data, certain large discrepancies exist between the two, most importantly, the drastic theoretical overestimation of the He^- and Li^- photodetachment cross sections just above their first K -shell thresholds. It was suggested [11,12] that this discrepancy was due to near-threshold recapture of photoelectrons and, indeed, this was independently verified [12] by using a classical correction to the quantum calculations for He^- , where the previous discrepancies between theory and experiment were resolved.

The present study describes how PCI can be incorporated quantum mechanically into the R -matrix formalism *via* an

optical potential approach. While equivalent methods have been proposed in the past [2,3,13–20], it was not clear how these results could be applied to an R -matrix calculation; the present approach grew out of the need to modify the coupled-channel R -matrix wave functions. We apply this method to the inner-shell photodetachment of Li^- and show that the previous discrepancies between theoretical and experimental results are now resolved.

Consider inner-shell photodetachment of Li^- leading to Li^+ production:

$$h\nu + \text{Li}^- (1s^2 2s^2) \rightarrow (1s 2s^2) \epsilon p_0 \quad (1)$$

$$\downarrow$$

$$(1s^2 \epsilon' s) \epsilon p_0$$

$$\begin{array}{cc} \swarrow & \searrow \\ \text{Li}^+ (1s^2) \epsilon p \epsilon' s & \text{Li} (1s^2 n p) \epsilon' s. \\ \text{(double detachment)} & \text{(recapture)} \end{array} \quad (2)$$

$$(3)$$

The photon is absorbed by a $1s$ electron [Eq. (1)], which propagates away from the neutral atom ($Z=0$) as a p wave with kinetic energy ϵ ; just above threshold, this photoelectron moves with a low velocity ($v = \sqrt{2\epsilon} \approx 0$) and has a strong shape resonance amplitude inside the $l=1$ angular-momentum barrier. Further $1s 2l' 2l''$ channels open up at higher photon energies due to strong correlation effects, but we focus only on the $1s 2s^2$ photodetachment channel.

The intermediate state $1s 2s^2 \epsilon p_0$ undergoes core Auger decay [Eqs. (1) and (2)] with rate Γ . The possible final states are given in Eq. (3). If the photoelectron has propagated sufficiently far from the neutral Li atom before the Auger decay occurs, then both the photoelectron and the Auger electron will escape to infinity, leaving Li^+ ions; these will be detected in the experiment. However, near threshold, where the photoelectron's velocity is small, the probability that the photoelectron will be recaptured once the emitted, faster Auger electron emerges and the photoelectron “sees” a positive Li^+ ionic core increases. Classically [18], using the sudden approximation, recapture occurs when the sum of the initial photoelectron kinetic energy and the ionic potential energy, $-1/r$, just after Auger decay, is less than zero, so that the photoelectron can no longer escape the Coulomb

attraction. Equivalently, the photoelectron could not have propagated beyond the classical turning point $r_c = 2/v^2$, in time $t_c = r_c/v = 2/v^3$, before the Auger decay occurred. The probability that the $1s2s^2$ state has *not* decayed in this time is given by $e^{-\Gamma t_c}$, so that the classical probability for escape of the photoelectron is given by $P_{class}^{esc} = e^{-2\Gamma/v^3}$. The photo-detachment partial cross section $\sigma_{1s \rightarrow \epsilon p_0}$ is multiplied by this probability to reflect the actual production of Li^+ ions. A similar classical method was used recently for the *total* He^- photodetachment cross section [12].

In principle, photoelectron recapture can be accounted for quantum mechanically by explicitly including the $1s^2np\epsilon's$ and $1s^2\epsilon p\epsilon's$ channels in the wave-function basis expansion. However, it is clearly impossible to include the entire np sequence for $n \rightarrow \infty$ explicitly, let alone the ϵp continuum; including only some becomes impractical even for states $n \leq 5$ due to the increasing R -matrix radius needed to contain these more diffuse states and the increased basis size needed. Usually, and indeed for the earlier R -matrix photo-detachment calculation of Li^- [5,10], only bound states up to about $n = 3$ can be explicitly included (which is sufficient for treating the initial photoabsorption process, but not the recapture process). That the $1s^2np\epsilon's$ and $1s^2\epsilon p\epsilon's$ channels originate from the Auger decay of the $1s2s^2\epsilon p_0$ channel, however, suggests the use of an optical potential [14,15,21] to implicitly include them.

A similar optical potential approach was used to account for spectator Auger decay of inner-shell *photoexcited* Rydberg states [22]. This method was found to give results in excellent agreement with the experimentally broadened resonance profiles seen in Ar [22], and later for Ne [23] and O [24]. Having established the validity of the optical potential R -matrix approach in those studies [22,25], we only describe the important features regarding core Auger decay of *continuum* (versus bound resonance) states.

In this calculation, we explicitly include all $1s^22l$, $1s^23l$, $1s2l2l'$, and $1s2s3l'$ target states of Li, coupled to an additional bound or free-electron orbital, in the R -matrix close-coupling expansion, as detailed in earlier studies [5,10]. The energies of the pertinent inner-shell vacancy target states are given in Table I. Following the Feshbach projection operator formalism [21], we partition our total wave function into a \mathcal{P} space of these explicitly included R -matrix channels and a \mathcal{Q} space of the infinite number of $1s^2(n, \epsilon)p\epsilon's$ channels accessible following the Auger decay of the core. The additional optical potential representing the influence of the \mathcal{Q} channels on the \mathcal{P} channels is then given by [21]

$$V_{opt} = H_{\mathcal{P}\mathcal{Q}}(E - H_{\mathcal{Q}\mathcal{Q}})^{-1}H_{\mathcal{Q}\mathcal{P}}, \quad (4)$$

where $H_{\mathcal{P}\mathcal{Q}} = \langle 1s2s^2|V|1s^2\epsilon's\rangle\langle\epsilon p_0|(n, \epsilon)p\rangle$, $V = \sum_{i \neq j} 1/r_{ij}$ is the interelectronic potential, and $H_{\mathcal{Q}\mathcal{Q}}$ is the Hamiltonian operator within \mathcal{Q} space. Since the ϵp_0 orbital sees no long-range potential, whereas the np and ϵp orbitals experience asymptotically a $Z=1$ Coulomb field, the overlap integrals $\langle\epsilon p_0|(n, \epsilon)p\rangle$ are nonzero in general. The optical potential, which has a small magnitude due to the small value of Γ , has

TABLE I. Energies [relative to the $\text{Li}^- 1s^22s^2(^1S)$ ground state] and Auger widths of the lowest Li $1s$ -vacancy states in LS coupling. The electron affinity of Li is computed as 0.628 eV compared to the experimental value of 0.618 eV [26].

State	$h\nu$ (eV)	$h\nu$ (eV)	Γ (meV)
	Present	Experiment	Present
$1s2s^2(^2S)$	56.934	56.968 ^a	36.76
$1s2s2p(^2P)$	59.494	59.528 ^b	3.48
$1s2s2p(^2P)$	61.008	61.014 ^b	9.54
$1s2p^2(^2D)$	61.681	61.680 ^a	10.63
$1s2p^2(^2P)$	62.206	62.235 ^a	0.0 ^c
$1s2s3s(^2S)$	62.554	62.610 ^a	8.20
$1s2s3p(^2P)$	62.990	63.037 ^b	0.20
$1s2s3d(^2D)$	63.459	63.517 ^a	1.06

^aReference [27] (including the electron affinity of 0.618 eV).

^bReference [28] (including the electron affinity of 0.618 eV).

^cRelativistically forbidden decay.

its main effect outside of the R -matrix box, where the continuum orbitals satisfy a modified equation

$$\left(H - \epsilon - i \frac{\Gamma}{2} \left[\sum_n |nl\rangle\langle nl| + \int d\bar{\epsilon} |\bar{\epsilon}l\rangle\langle \bar{\epsilon}l| \right] \right) |\epsilon p_0\rangle = 0; \quad (5)$$

here the asymptotic one-electron Hamiltonian operator at large r is given by $Hf_{\epsilon l}(r) = (-\frac{1}{2}(d^2/dr^2) + \frac{1}{2}[l(l+1)/r^2])f_{\epsilon l}(r)$, and the width is $\Gamma = 2\pi \langle 1s2s^2|V|1s^2\epsilon's\rangle^2$. The two terms in the square brackets in Eq. (5) are projection operators onto the bound np and continuum ϵp states, respectively, acting on the ϵp_0 function. By the closure relation, assuming that the ϵp_0 orbital can be completely spanned by the nl and ϵl functions, the sum of the two projection operators is the identity operator, and Eq. (5) becomes

$$\left(-\frac{1}{2} \frac{d^2}{dr^2} + \frac{1}{2} \frac{l(l+1)}{r^2} - \left[\epsilon + i \frac{\Gamma}{2} \right] \right) f_{\epsilon l}(r) = 0. \quad (6)$$

The solutions of Eq. (6) are the Riccati Bessel and Neumann functions $j_l(kr)$ and $n_l(kr)$, where $k = \sqrt{2\epsilon + i\Gamma} = k_R + ik_I$, and the inner-region R -matrix solution can be matched to these to yield scattering and dipole matrices. This can be done for the multichannel case just as easily.

The *final*-state wave function [29], after photoabsorption, for the outgoing solution in each channel, outside the R -matrix box, is a Riccati Hankel function $h_l^{(1)}(kr) = j_l(kr) + i n_l(kr)$ (inside it has a more complicated behavior, being a solution to a coupled-channel inhomogeneous differential equation—see Eq. (28) of Ref. [29]). Each solution has $r \rightarrow \infty$ asymptotic form $e^{+ikr} \sim e^{-k_I r}$, decaying exponentially for $\Gamma > 0$. The physical interpretation of this solution is straightforward: the initially photoabsorbed (\mathcal{P} -space) wave packet propagates outward from the atom in an absorbing optical potential $-i\Gamma/2$, but never reaches $r \rightarrow \infty$. Instead, the atom decays into \mathcal{Q} space, producing an Auger electron

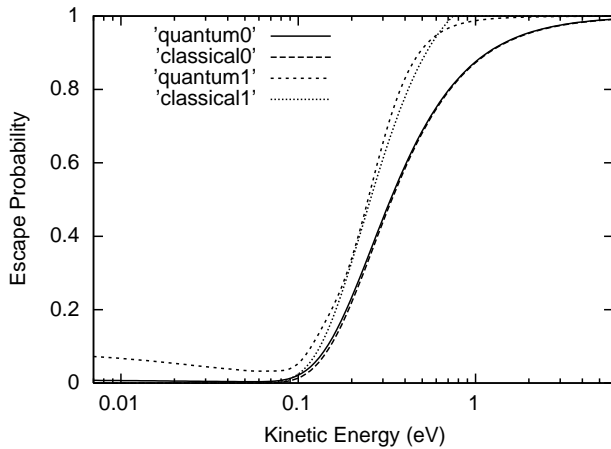


FIG. 1. Comparison between quantum and classical escape probabilities following core Auger decay (with $\Gamma = 36.8$ meV); the two cases ($l=0$, $a=0$) and ($l=1$, $a=35.4$ a.u.) are shown.

and an intermediate photoelectron state ϵp_0 coupled to the Li^+ core. The probability of decaying to the Li states is given by the projection of the ϵp_0 orbital onto the bound Coulomb orbitals $P_{\text{quan}}^{\text{recap}} = (\sum_n |\langle \epsilon p_0 | np \rangle|^2) / \langle \epsilon p_0 | \epsilon p_0 \rangle$, and the probability of decaying instead to ionized Li^+ states is given by

$$P_{\text{quan}}^{\text{esc}} = 1 - P_{\text{quan}}^{\text{recap}}. \quad (7)$$

The partial cross sections for ejection of an electron in each channel are then multiplied by $P_{\text{quan}}^{\text{esc}}$ to yield the measured Li^+ ion yield from each channel. Table I lists the computed Auger widths for each of the Li inner-shell vacancy states in the region of interest.

In order to investigate the energy dependence of the escape probability, we assume that the outgoing electron orbital is simply a Hankel function outside of the *R*-matrix box ($r > a$) and is zero inside. The overlaps in Eq. (7) then take the form of integrals $\langle \epsilon p_0 | np \rangle = \int_a^\infty h_l^{(1)*}(kr) \phi_{nl}(r) dr$, where $\phi_{nl}(r)$ are the Coulomb bound-state solutions. Since the Hankel and Coulomb functions are expressible as finite expansions of the form $\sum_j c_j r^j e^{-br}$, we can evaluate the integrals analytically. The quantum and classical escape probabilities are shown in Fig. 1 for the two cases ($l=0, a=0$) and ($l=1, a=35.4$); the latter is chosen to represent the $1s2s^2\epsilon p_0$ channel, with the actual *R*-matrix box size of 35.4 a.u., and Auger width $\Gamma = 36.76$ meV from Table I. The classical formula for $l > 0$ and $a > 0$ has been modified slightly to include only recapture over the region $a \leq r \leq r_c$, and the classical turning point is now computed including the angular-momentum potential as $r_c = [1 + \sqrt{1 - 2\epsilon l(l+1)}] / 2\epsilon$.

It can be seen in Fig. 1 that for $l=0$ and $a=0$ the agreement between the quantum and classical escape probabilities is quite close (a similar comparison is found in Ref. [20]). Only at the lowest energies does the computed quantum-mechanical result differ from the classical one, not quite going to zero. This is most likely due to our approximation of setting the ϵp_0 orbital to be a Hankel function for all r with

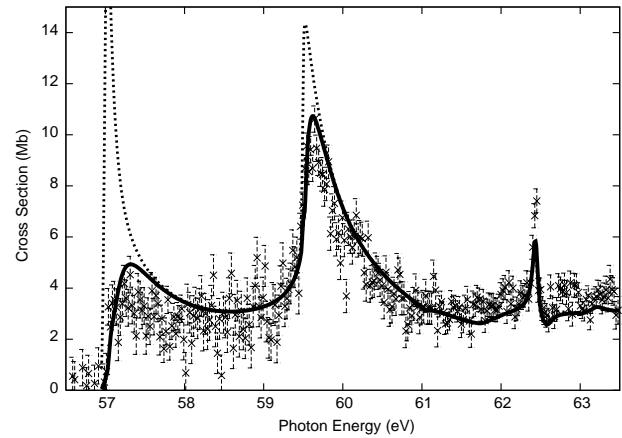


FIG. 2. Photodetachment of Li^- yielding Li^+ ions. The experimental results from Ref. [5] (crosses, shifted by -0.165 eV) are compared to the standard *R*-matrix results (dotted line) and the optical potential results (solid line).

the incorrect boundary condition $h_0^{(1)}(0) \neq 0$. Therefore, these approximate functions cannot be spanned by the physical np and ϵp functions, which vanish at $r=0$, so the closure relation breaks down. The low-energy difference between our quantum results, using approximate functions, and the classical results becomes worse for $l > 0$ (and necessarily $a > 0$), where the exponentially diverging solutions for $r \rightarrow 0$ are approximated even more poorly by the np and ϵp functions; the escape probability remains at about 0.1 rather than going to zero. We could use more sophisticated outgoing solutions, but would then lose the analytic expressions for determining the overlap integrals.

Given the computed escape probabilities in each channel P_i^{esc} , which depend only on the energy ϵ_i , the angular momentum l_i , and the core Auger width Γ_i (given in Table I), we can obtain an expression for the Li^+ cross sections as

$$\sigma(\text{Li}^+) = \sum_{i \in \text{Auger}} P_i^{\text{esc}} \sigma_i, \quad (8)$$

where σ_i is the partial *R*-matrix photodetachment cross section to channel i , and the sum includes only those channels i which can core Auger decay.

The computed cross section for Li^+ production is shown in Fig. 2 compared to the standard *R*-matrix results and experiment [5]. The biggest effect of including the photoelectron recapture process is the drastic reduction in the cross section just above the $1s2s^2$ threshold at 56.934 eV, which is now in excellent agreement with experiment. Note that the core Auger decay width for this state is $\Gamma = 36.76$ meV $= 1.35 \times 10^{-3}$ a.u., so by the expression for $P_{\text{class}}^{\text{esc}} = e^{-2\Gamma/(2\epsilon)^{3/2}}$, we expect a significant reduction within about $\epsilon \approx 2\Gamma^{2/3} = 0.0244$ a.u. $= 0.67$ eV above threshold, and indeed this is the case. At the next threshold, $1s(2s2p[{}^3P])({}^2P)$ at 59.494 eV, the reduction is less pronounced due to the smaller Auger width of 3.48 meV. The shape resonance cross section computed with the optical potential method is again in excellent agreement with the experimental result and is the dominant feature seen in Fig. 2.

The only other feature clearly discernable in the experimental results is the narrow resonance at 62.4 eV, also seen in the present R -matrix results. This resonance is above the $1s2p^2(^2P)$ state of Li, which cannot Auger decay to any $1s^2\epsilon l$ continua in LS coupling, so the cross section here cannot be reduced by photoelectron recapture.

In conclusion, we have shown that an optical potential approach can be used in conjunction with the R -matrix method to include the postcollision recapture process. The calculation for the K -shell photodetachment cross section of Li^- yielding Li^+ shows a dramatic reduction of the large shape resonance above the first threshold, bringing theoretical and experimental results into excellent agreement and explaining the earlier, large discrepancies between the two

[5]. Our R -matrix approach allows for the inclusion of the crucial channel-coupling effects as well as the separation into individual channel components. Using this formulation including PCI gives not only the total cross section, but partial cross sections as well, which provides more detailed information on the postcollision interaction between the photoelectron and the Auger electron.

Discussions with F. Robicheaux, N. R. Badnell, and E. Lindroth are gratefully acknowledged. T.W.G. and O.Z. were supported by NASA. H.L.Z. and S.T.M. were supported by NSF and NASA. Z.F. and A.Z.M. were supported by U.S. DOE, Division of Chemical Sciences, Office of Basic Energy Research and NSF.

-
- [1] S.J. Buckman and C.W. Clark, *Rev. Mod. Phys.* **66**, 539 (1994), and references therein.
- [2] A. Russek and W. Mehlhorn, *J. Phys. B* **19**, 911 (1986), and references therein.
- [3] M. Yu Kuchiev and S.A. Sheinerman, *J. Phys. B* **18**, L551 (1985).
- [4] N. Berrah, J.D. Bozek, G. Turri, G. Akerman, B. Rude, H.L. Zhou, and S.T. Manson, *Phys. Rev. Lett.* **88**, 093001 (2002).
- [5] N. Berrah, J.D. Bozek, A.A. Wills, G. Turri, H.-L. Zhou, S.T. Manson, G. Akerman, B. Rude, N.D. Gibson, C.W. Walter, L. VoKy, A. Hibbert, and S.M. Ferguson, *Phys. Rev. Lett.* **87**, 253002 (2001).
- [6] H. Kjeldsen, P. Andersen, F. Folkmann, B. Kristensen, and T. Andersen, *J. Phys. B* **34**, L353 (2001).
- [7] N.D. Gibson, C.W. Walter, O. Zatsarinny, T.W. Gorczyca, G.D. Ackerman, J.D. Bozek, M. Martins, B.M. McLaughlin, and N. Berrah, *Phys. Rev. A* **67**, 030703(R) (2003).
- [8] P.G. Burke and K.A. Berrington, *Atomic and Molecular Processes: An R-matrix Approach* (IOP, Bristol, 1993).
- [9] O. Zatsarinny, T.W. Gorczyca, and C. Froese Fischer, *J. Phys. B* **35**, 4161 (2002).
- [10] H.-L. Zhou, S.T. Manson, L. VoKy, N. Feautrier, and A. Hibbert, *Phys. Rev. Lett.* **87**, 023001 (2001).
- [11] M. Ya. Amusia (private communication).
- [12] J.L. Sanz-Vicario, E. Lindroth, and N. Brandefelt, *Phys. Rev. A* **66**, 052713 (2002).
- [13] G.C. King, F.H. Read, and R.C. Bradford, *J. Phys. B* **8**, 2210 (1975).
- [14] C. Bottcher and K.R. Schneider, *J. Phys. B* **9**, 911 (1976).
- [15] G. Niehaus and H.G.M. Heidemann, *J. Phys. B* **9**, 2053 (1976).
- [16] A. Niehus, *J. Phys. B* **10**, 1845 (1977).
- [17] G.B. Armen, J. Tulkki, T. Åberg, and B. Craseman, *Phys. Rev. A* **36**, 5606 (1987).
- [18] J. Tulkki, T. Åberg, S.B. Whitfield, and B. Craseman, *Phys. Rev. A* **41**, 181 (1990).
- [19] M. Ya. Amusia, *Atomic Photoeffect* (Plenum, New York, 1990).
- [20] G.B. Armen and J.C. Levin, *Phys. Rev. A* **56**, 3734 (1997).
- [21] H. Feshbach, *Ann. Phys. (N.Y.)* **5**, 357 (1958); **19**, 287 (1962).
- [22] T.W. Gorczyca and F. Robicheaux, *Phys. Rev. A* **60**, 1216 (1999).
- [23] T.W. Gorczyca, *Phys. Rev. A* **61**, 024702 (2000).
- [24] T.W. Gorczyca and B.M. McLaughlin, *J. Phys. B* **33**, L859 (2000).
- [25] F. Robicheaux, T.W. Gorczyca, M.S. Pindzola, and N.R. Badnell, *Phys. Rev. A* **52**, 1319 (1995).
- [26] G. Haefliger, D. Hanstorp, I. Kiyani, A.E. Klinkmüller, U. Ljungblad, and D.J. Pegg, *Phys. Rev. A* **53**, 4127 (1996).
- [27] D.L. Ederer, T. Lucatorto, and R.P. Madden, *Phys. Rev. Lett.* **30**, 1537 (1970).
- [28] T.J. McIlrath and T.B. Lucatorto, *Phys. Rev. Lett.* **38**, 1390 (1977).
- [29] F. Robicheaux, *Phys. Rev. A* **48**, 4162 (1993).